Clin Cancer Res, revised version

Histone deacetylase 3 inhibition overcomes *BIM* deletion polymorphism-mediated osimertinib-resistance in *EGFR*-mutant lung cancer

Azusa Tanimoto [1], Shinji Takeuchi [1], Sachiko Arai [1], Koji Fukuda [1], Tadaaki Yamada [1], Xavier Roca [2], S. Tiong Ong [3, 4, 5, 6], Seiji Yano [1]

[1] Divisions of Medical Oncology, Cancer Research Institute, Kanazawa University, Kanazawa, Japan

[2] School of Biological Sciences, Nanyang Technological University, Singapore

[3] Cancer & Stem Cell Biology Signature Research Programme, Duke-NUS Medical School, Singapore

[4] Department of Medical Oncology, National Cancer Centre Singapore, Singapore

[5] Department of Haematology, Singapore General Hospital, Singapore

[6] Department of Medicine, Duke University Medical Center, Durham NC, USA

Running title: HDAC3 inhibition and EGFR-TKI resistance by *BIM* polymorphism

Keywords: *EGFR* mutation, osimertinib, *BIM* polymorphism, HDAC3, apoptosis

Financial support: This work was supported by JSPS KAKENHI Grant Number JP16H05308 (to SY), the Project for Cancer Research And Therapeutic Evolution (P-CREATE) Grant Number 16cm0106513h0001 (to SY), and grants from the Japan Agency for Medical Research and Development, AMED, Grant Number 15Aak0101016h0003 15Ack0106113h0002 and (to SY). XR and STO were supported by the Singapore Ministry of Health's National Medical Research Council under its Clinician Scientists Individual Research Grant (NMRC/CIRG/1330/2012), and STO by the Clinician Scientist Award (NMRC/CSA/0051/2013), administered by the Singapore

Ministry of Health's National Medical Research Council.

Corresponding Author: Seiji Yano, MD, PhD. Division of Medical Oncology Cancer Research Institute, Kanazawa University 13-1, Takaramachi, Kanazawa, Ishikawa, 920-0934, Japan

Phone: +81- 76-265-2794, Fax: +81- 76-244-2454 E-mail: syano@staff.kanazawa-u.ac.jp

Conflict of Interest Disclosure: Seiji Yano obtained research grants from AstraZeneca, Chugai Pharma, and Boehringer-Ingelheim, and honoraria from Chugai Pharma and Boehringer-Ingelheim. The other authors have no conflict of interest.

Abstract

Purpose : The *BIM* deletion polymorphism is associated with apoptosis resistance to epidermal growth factor receptor tyrosine kinase inhibitors (EGFR-TKIs), such as gefitinib and erlotinib, in non-small cell lung cancer (NSCLC) harboring *EGFR* mutations. Here, we investigated whether the *BIM* deletion polymorphism contributes to resistance against osimertinib, a third-generation EGFR-TKI. In addition, we determined the efficacy of a histone deacetylase (HDAC) inhibitor, vorinostat, against this form of resistance and elucidated the underlying mechanism.

Experimental Design : We used *EGFR*-mutated NSCLC cell lines which were either heterozygous or homozygous for the *BIM* deletion polymorphism to evaluate the effect of osimertinib *in vitro* and *in vivo*. Protein expression was examined by western blotting. Alternative splicing of *BIM* mRNA was analyzed by RT-PCR.

Results : *EGFR*-mutated NSCLC cell lines with the *BIM* deletion polymorphism exhibited apoptosis resistance to osimertinib in a polymorphism dosage-dependent manner, and this resistance was overcome by combined use with vorinostat. Experiments with homozygous *BIM* deletion-positive cells revealed that vorinostat affected the alternative splicing of *BIM* mRNA in the deletion allele, increased the expression of active BIM protein, and thereby induced apoptosis in osimertinib-treated cells. These effects were mediated predominantly by HDAC3 inhibition. In xenograft models, combined use of vorinostat with osimertinib could regress tumors in *EGFR*-mutated NSCLC cells homozygous for the *BIM* deletion polymorphism. Moreover, this combination could induce apoptosis even when tumor cells acquired *EGFR*-T790M mutations.

Conclusions : These findings indicate the importance of developing HDAC3-selective inhibitors, and their combined use with osimertinib, for treating *EGFR*-mutated lung cancers carrying the *BIM* deletion polymorphism.

Translational Relevance

Patients with *EGFR*-mutated NSCLC who also harbor the *BIM* deletion polymorphism, experience shorter progression-free survival when treated with first-generation EGFR-TKIs, gefitinib and erlotinib. While we recently reported that the HDAC inhibitor, vorinostat, could overcome EGFR-TKI resistance mediated by the *BIM* deletion polymorphism in *EGFR*-mutated NSCLC cells, the specific target of vorinostat was unknown. In the present study, we confirm that the *BIM* deletion polymorphism is sufficient to confer resistance to first–generation EGFR-TKIs as well the third-generation TKI, osimertinib. We further identified HDAC3 as an important regulator of *BIM* pre-mRNA splicing, and that the activity of vorinostat is likely to require inhibition of HDAC3. Our findings illustrate the importance of developing selective HDAC3 inhibitors, and provide the rationale for combined use of HDAC3 inhibitors with osimertinib in patients with *EGFR*-mutated NSCLC who carry the *BIM* deletion polymorphism.

Introduction

The majority of patients with non-small cell lung cancer (NSCLC) with epidermal growth factor receptor (EGFR) activating mutations, such as exon 19 deletion and L858R point mutation, show marked responses to the first-generation reversible EGFR tyrosine kinase inhibitors (EGFR-TKIs), gefitinib and erlotinib (1, 2). However, the acquisition of TKI resistance is almost inevitable, and is commonly associated with the so-called *EGFR*-T790M gatekeeper mutation, which substitutes a threonine with a methionine at the amino acid position 790 of exon 20. Accordingly, the T790M mutation is detected in 50–60% of patients who develop clinical resistance to the first generation EGFR-TKIs, gefitinib or erlotinib (3, 4).

Osimertinib, a mono-anilino-pyrimidine compound, is a third-generation irreversible EGFR-TKI, which has activity against EGFR with sensitizing mutations, such as the exon 19 deletion, L858R mutation, and T790M resistance mutation, but spares wild-type EGFR (5). While the second-generation irreversible EGFR-TKI, afatinib, can inhibit the T790M mutation *in vitro*, it also has high activity against wild type EGFR and has failed to demonstrate an objective response rate (ORR; less than 10%) in NSCLC patients with the *EGFR*-T790M mutation (6). In contrast, osimertinib exhibited a prominent anticancer effect (confirmed ORR, 61%) among an equivalent cohort of patients (7), and was thus approved for the treatment of patients harboring the T790M mutation in Europe, the United States, and Japan.

BIM, also called Bcl-2-like protein 11, is a pro-apoptotic molecule that belongs to the Bcl-2 family. BIM upregulation is essential for the induction of apoptosis in lung cancer cells with *EGFR* mutations treated with first-generation EGFR-TKIs, and low BIM protein level is associated with resistance to EGFR-TKIs (8, 9). In East Asians but not Caucasians or Africans, a 2,903 kb deletion polymorphism in the *BIM* gene was found to be present at incidences of around 13% and 0.5% for heterozygous and homozygous carriers respectively (10). Another study has recently reported that 15.7% of hispanic patients with NSCLC carried the deletion allele (11). Importantly, the *BIM* deletion polymorphism results in the preferential splicing of exon 3 over the BH3-encoding exon 4 in the *BIM* pre-mRNA, and leads to the production of inactive BIM isoforms lacking the BH3 domain. This in turn reduces expression of pro-apoptotic BIM protein isoforms in *EGFR*-mutated lung cancer cell lines following TKI exposure, and is sufficient to confer TKI resistance (10). The polymorphic fragment includes multiple and redundant splicing silencers that repress exon 3 inclusion (12). Since its initial discovery, several meta-analyses have reported the association between *BIM* deletion polymorphism and shorter progression-free survival (PFS) of patients with NSCLC harboring *EGFR*

mutations, who received gefitinib or erlotinib treatment (13). However, it is unknown if the *BIM* deletion polymorphism affects the anti-tumor efficacy of third generation EGFR-TKIs including osimertinib.

We previously reported that the combined use of gefitinib and the histone deacetylase (HDAC) inhibitor, vorinostat, was able to preferentially upregulate the expression of pro-apoptotic BIM isoforms in *EGFR*-mutated NSCLC cell lines heterozygous for the *BIM* deletion, and overcome EGFR-TKI resistance *in vitro* and *in vivo* (14). However, it remained unclear how vorinostat corrected the splicing defect conferred by the *BIM* deletion, and if vorinostat could overcome resistance in the setting of cells with homozygous *BIM* deletions.

In the present study, we examined the ability of osimertinib, in comparison to afatinib and gefitinib, to induce apoptosis in *EGFR*-mutated lung cancer cell lines with either heterozygous or homozygous configurations of the *BIM* deletion polymorphism. We also determined the effect of vorinostat on *BIM* deletion polymorphism-mediated resistance to osimertinib both *in vitro* and *in vivo*. We further identified the target HDAC molecule whose inhibition can overcome EGFR-TKI-resistance in *EGFR*-mutated lung cancer cells bearing the *BIM* deletion polymorphism.

Materials and Methods

Cell lines and reagents

NSCLC cell lines PC-9 and PC-3, which have an exon 19 deletion in the *EGFR*, were obtained from Immuno-Biological Laboratories Co., ltd. (Gumma, Japan) in May 2015, and Human Science Research Resource Bank (Osaka, Japan) in March 2013, respectively (14). PC-9 cells with a homozygous *BIM* deletion polymorphism (PC-9*BIM*$^{\Delta 2/\Delta}$), were established by editing with zinc finger nuclease, as reported previously (10). All three cell lines were subcultured in RPMI-1640 medium supplemented with 10% FBS and antibiotics within 3 months of thawing the frozen stock. Mycoplasma infection in the cells was regularly checked using a MycoAlert Mycoplasma Detection Kit (Lonza, Basel, Switzerland). The cell line authentication was performed by short tandem repeat analysis at the laboratory of the National Institute of Biomedical Innovation (Osaka, Japan) in May 2015. Gefitinib, afatinib, osimertinib, vorinostat, belinostat, droxinostat, and RGFP966 were obtained from Selleck Chemicals (Houston, TX). All drugs were dissolved in DMSO and preserved at 30 °C.

Genotyping of *BIM* deletion polymorphism

Cellular DNAs were extracted from the cells using a DNeasy Blood and Tissue Kit (Qiagen, Velno, the Netherlands). To recognize the presence of the wild-type and deletion alleles, we conducted PCR reactions using the discriminating primers for the wild-type alleles (forward: 5′-CCACCAATGGAAAAGGTTCA-3′; reverse: 5′-CTGTCATTTCTCCCCACCAC-3′) and deletion alleles (forward: 5′-CCACCAATGGAAAAGGTTCA-3′; reverse: 5′-GGCACAGCCTCTATGGAGAA-3′). The genomic DNAs were amplified using a Veriti Thermal Cycler (Applied Biosystems, Waltham, MA) with GoTaq Hot Start Polymerase (Promega, Fitchburg, WI). The PCR amplicons for the wild-type (362 bp) and the deletion (284 bp) alleles were separated by agarose gel electrophoresis.

Cell apoptosis assay

Cellular apoptosis induced by the drugs was determined through the use of a FACSCalibur flow cytometer (BD Biosciences, San Diego, CA) with a PE Annexin V Apoptosis Detection Kit I (BD Biosciences), which detects and quantifies apoptotic cells with phycoerythrin (PE) Annexin V and 7-amino-actinomycin (7-AAD) staining.

Western blotting

The proteins harvested were separated via sodium dodecyl sulfate polyacrylamide gel

electrophoresis (SDS-PAGE). The proteins were transferred onto polyvinylidene fluoride membranes (Bio-Rad, Hercules, CA), which were immersed in StartingBlock T20 (TBS) Blocking Buffer (Thermo Fisher Scientific, Waltham, MA) for 1 hour at about 20 °C, followed by incubation above 8 hours at 4 °C with antibodies against phospho-EGFR (Tyr1068), Akt, phospho-Akt (Ser473), cleaved PARP, cleaved caspase-3, histone H3, acetylated histone H3 (Lys27), BIM, and β-actin (Cell Signaling Technology, MA); and against phospho-Erk1/2 (Thr202/Tyr204), Erk1/2, and EGFR (R&D Systems, Minneapolis, MN). After washing three times in the tris buffered saline with the polyoxyethylene sorbitan monolaurate (TBST), the membranes were incubated for 1 hour at room temperature with horseradish peroxidase-conjugated secondary antibodies. The proteins labeled with secondary antibodies were visualized using SuperSignal West Dura Extended Duration Substrate Enhanced Chemiluminescent Substrate (Thermo Fisher Scientific). Each experiment was independently carried out at least three times.

RNA interference

The cells (1×10^5) cultured in medium containing 10% FBS (antibiotic free) for 24 hours were treated with Stealth RNAi siRNA against *BIM* and *HDAC* 1, 2, 3, 6, and Stealth RNAi siRNA Negative Control Lo GC (Invitrogen, Carlsbad, CA) using Lipofectamine RNAiMAX (Invitrogen) for 48 hours.

Real-time quantitative reverse transcription PCR

Total cellular RNAs were extracted from the cells using RNeasy PLUS Mini kit (Qiagen). Reverse transcription of the collected RNAs was performed using SuperScript VILO cDNA synthesis Kit and Master Mix (Invitrogen). Expression of *BIM* mRNA was quantitatively measured by ViiA 7 Real-Time PCR System (Applied Biosystems, Framingham, MA) using the following primers: *BIM* exon 2A (forward: 5′-ATGGCAAAGCAACCTTCTGATG-3′; reverse: 5′-GGCTCTGTCTGTAGGGAGGT-3′), *BIM* exon 3 (forward: 5′-CAATGGTAGTCATCCTAGAGG-3′; reverse: 5′-GACAAAATGCTCAAGGAAGAGG-3′), *BIM* exon 4 (forward: 5′-TTCCATGAGGCAGGCTGAAC-3′; reverse: 5′-CCTCCTTGCATAGTAAGCGTT-3′) and β-actin (forward: 5′-GGACTTCGAGCAAGAGATGG-3′; reverse: 5′-AGCACTGTGTTGGCGTACAG-3′).

Xenograft studies

Male 5- to 6-week-old BALB/c-nu/nu mice were injected subcutaneously into both flanks with cultured tumor cells (5×10^6 cells/0.1 mL/mouse). After tumor volumes reached 80 to 100 mm^3, the mice were randomized and treated once daily by oral gavage with osimertinib and/or vorinostat. Each tumor was monitored using an electronic caliper. Tumor volume was measured in two dimensions, and calculated using the following formula: tumor volume (mm^3) = 1/2 × length (mm) × width $(mm)^2$. After mice were treated for 4 days, 2 tumors in each control and treatment group were excised, lysed, and subjected to western blot analysis. All animal experiments were complied with the Guidelines for the Institute for Experimental Animals, Kanazawa University Advanced Science Research Center (approval No. AP-081088).

Statistical analysis

Differences between groups were analyzed by one-way ANOVA. All statistical analyses were conducted using Graph-Pad Prism Ver. 6.05 (GraphPad Software Inc, San Diego, CA). The threshold for significance was $P < 0.05$.

Results

BIM deletion polymorphism-positive NSCLC cells with *EGFR* mutations are resistant to third-generation EGFR-TKIs

We first carried out PCR to confirm the presence of the *BIM* deletion polymorphism in *EGFR*-mutated NSCLC cell lines. PC-9 cells did not harbor the *BIM* deletion, but as expected, PC-3 and PC-9*BIM*$^{\Delta 2/-}$ cells were heterozygous and homozygous for the deletion, respectively (Fig. 1A) (10, 14). Next, we assessed the degree of apoptosis induction by second- and third-generation EGFR-TKIs in these cell lines. Using a FACS-based assay, we found that both afatinib and osimertinib induced significant apoptosis in PC-9 cells, but not in PC-3 or PC-9*BIM*$^{\Delta 2/-}$ cells (Fig. 1B). Western blot analyses for cleaved PARP and caspase-3 confirmed low apoptosis induction in PC-3 and PC-9*BIM*$^{\Delta 2/-}$ cells, in contrast to PC-9 cells, when treated with gefitinib, afatinib, and osimertinib. All three EGFR-TKIs inhibited EGFR phosphorylation, as well as its downstream kinases AKT and ERK, in PC-9, PC-3, and PC-9*BIM*$^{\Delta 2/-}$ cells. While the EGFR-TKIs induced active BIM (BIM_{EL}) protein in PC-9 cells, the level of BIM_{EL} protein in EGFR-TKI-treated PC-3 and PC-9*BIM*$^{\Delta 2/-}$ cells was much lower (Fig. 1C). Moreover, knockdown of BIM protein by *BIM*-specific siRNA resulted in the abrogation of apoptosis, as shown by the absence of cleaved PARP and cleaved caspase-3 in EGFR-TKI-treated PC-9 cells (Fig. 1D). These results clearly indicate that the presence of the *BIM* deletion polymorphism, in one or both alleles, is sufficient to mediate resistance to all three generations of EGFR-TKIs in *EGFR*-mutated NSCLC cells.

Combined use of second- or third-generation EGFR-TKIs and an HDAC inhibitor enhances BIM expression and induces apoptosis

We previously reported that the combined use of an HDAC inhibitor, vorinostat, with gefitinib induces apoptosis in *EGFR*-mutated NSCLC cells harboring a single allele of the *BIM* deletion polymorphism. We therefore investigated the effect of vorinostat combined with second- or third-generation EGFR-TKIs on apoptosis induction in PC-3 and PC-9*BIM*$^{\Delta 2/-}$ cells. Consistent with the results shown in Fig. 1C, afatinib or osimertinib alone induced very low levels of BIM_{EL}, cleaved PARP, and cleaved caspase-3 in PC-3 and PC-9*BIM*$^{\Delta 2/-}$ cells, while at the same time, completely inhibited EGFR phosphorylation and its downstream targets, AKT and ERK (Fig. 2A). Meanwhile, combined use of vorinostat with either afatinib or osimertinib markedly up-regulated BIM_{EL} expression, and thus induced cleaved PARP and cleaved caspase-3 (Fig. 2A). Moreover, knockdown of the BIM protein by *BIM*-specific siRNA resulted in the inhibition of apoptosis induced by vorinostat, combined with afatinib or osimertinib,

in PC-9*BIM*$^{\Delta 2/\Delta 2}$ cells (Fig. 2B). These results indicate that vorinostat overcame apoptosis resistance to second- and third-generation EGFR-TKIs by inducing active BIM protein (BIM_{EL}) expression in *EGFR*-mutated NSCLC cells with are either heterozygous or homozygous for the *BIM* deletion polymorphism.

HDAC3 inhibition leads to the upregulation of active BIM protein

Vorinostat is a non-specific HDAC inhibitor, and targets both class I HDACs (HDAC 1, 2, 3, and 8) and class II HDACs (HDAC 6 and 10) (15). Considering the various side effects of vorinostat (16), a selective HDAC inhibitor may bring about less toxicity in combination with osimertinib. To elucidate which HDAC plays a role in the induction of active BIM protein expression and cell death, we treated PC-9*BIM*$^{\Delta 2/\Delta 2}$ cells with specific siRNA for HDAC 1, 2, 3, or 6. Interestingly, HDAC3 knockdown induced up-regulation of *BIM* exon 4-containing transcripts that encode pro-apoptotic BH3-containing (active) BIM isoforms (Fig. 3A, 3B and Supplementary Fig. S1). Moreover, knockdown of HDAC3 restored active BIM protein expression and induced apoptosis by osimertinib in PC-3 and PC-9*BIM*$^{\Delta 2/\Delta 2}$ cells (Fig. 3C). These results strongly suggest that HDAC3 inhibition is important for the transcription of *BIM* exon 4-containing isoforms, and is sufficient for the induction of active BIM protein isoforms, including BIM_{EL}. This was further supported by the results of other HDAC inhibitors with different HDAC inhibitory profiles. Droxinostat, an HDAC inhibitor under development, has much weaker inhibitory activity against HDAC3 compared to vorinostat (IC_{50} values of HDAC3 inhibition by droxinostat and vorinostat are 16.9 ± 5.0 μM and 20 nM, respectively) (17, 18). At equivalent concentrations, droxinostat, in contrast to vorinostat, failed to significantly upregulate active BIM protein, and was unable to induce apoptosis in PC-9*BIM*$^{\Delta 2/\Delta 2}$ cells even in combination with osimertinib (Fig. 3D). We also tested belinostat, a pan-HDAC inhibitor (IC_{50} value of HDAC3 inhibition is 27 nM) whose inhibitory profile is similar to that of vorinostat (19), and which is approved for the treatment of relapsed or refractory peripheral T-cell lymphoma (PTCL) by the Food and Drug Administration (FDA). As is the case with vorinostat, combined use of belinostat and EGFR-TKIs (gefitinib, afatinib, and osimertinib) enhanced the expression of active BIM, and induced apoptosis in PC-3 and PC-9*BIM*$^{\Delta 2/\Delta 2}$ cells (Supplementary Fig. S2A). Furthermore, a selective HDAC3 inhibitor, RGFP966 (IC_{50} value of HDAC3 inhibition is 80nM) (20), clearly induced apoptosis in combination with osimertinib together with up-regulating active BIM in PC-9*BIM*$^{\Delta 2/\Delta 2}$ cells (Supplementary Fig. S2B). These findings implicate HDAC3 inhibition as an important target in the ability of vorinostat to induce apopotosis in *EGFR*-mutated NSCLC cells

with the *BIM* deletion polymorphism.

Vorinostat affects splicing in the deletion allele of *BIM* predominantly via HDAC3 inhibition

In our previous study which employed heterozygous *BIM* deletion-positive NSCLC (PC-3) cells with *EGFR* mutations, vorinostat preferentially induced the expression of the exon 4-containing isoform (encoding BH3-domain containing BIM), although its exact mechanisms of action remain unclear. There are two possibilities to explain this observation: 1) vorinostat up-regulated the transcription of the exon 4-containing isoform from either or both *BIM* alleles, or 2) vorinostat affected *BIM* splicing, resulting in the production of exon 4 rather than exon 3-containing transcripts from the deletion polymorphism allele. To elucidate the mechanism, we evaluated the ratio of exon 3 to exon 4 transcripts in PC-9*BIM*$^{\Delta 2/\Delta 2}$ cells (homozygous *BIM* deletion), compared to those in PC-3 (heterozygous *BIM* deletion) and PC-9 (with only full-length *BIM* alleles) cells. As reported previously, the ratio of exon 3 to exon 4 transcripts in PC-3 cells was higher than that in PC-9 cells. As expected, the ratio of exon 3 to exon 4 transcripts in PC-9*BIM*$^{\Delta 2/\Delta 2}$ cells was also higher than in PC-3 cells (Supplementary Fig. S3A). In PC-9*BIM*$^{\Delta 2/\Delta 2}$cells, vorinostat up-regulated the transcription of the exon 4-containing isoform (Fig. 4A), which was further enhanced in combination with the EGFR-TKI gefitinib or osimertinib (Fig. 4A and Supplementary Fig. S3B). Vorinostat markedly decreased the ratio of exon 3 to exon 4 transcripts compared to the control (Fig. 4B). These results indicate that vorinostat affected the splicing process in the *BIM* deletion allele, rather than the full-length allele.

We next sought to elucidate whether HDAC3 inhibition prominently affects the alternative splicing of *BIM* pre-mRNA. Knockdown of HDAC3 elevated the mRNA expression of exon 2A and exon 4, and thus strongly decreased the ratio of exon 3 to exon 4 transcripts (Fig. 4C). While droxinostat (which weakly inhibits HDAC3) did not significantly decrease the ratio of exon 3 to exon 4 transcripts, RGFP966 with selective inhibitory activity to HDAC3 did decrease it (Supplementary Fig. S4A and S4B). These findings suggest that HDAC3 inhibition contributes to the alternative splicing of *BIM* by promoting exon 4 inclusion.

Vorinostat combined with osimertinib regresses tumors with homozygous *BIM* deletion polymorphism in *EGFR*-mutated NSCLC cells *in vivo*

We next examined the effect of combination therapy with osimertinib and vorinostat on *EGFR*-mutated NSCLC cells homozygous for the *BIM* deletion polymorphism *in vivo*. PC-9*BIM*$^{\Delta 2/\Delta 2}$tumor-bearing mice were treated with osimertinib, vorinostat, or a

combination of both. In contrast to PC-9 xenograft tumors which decreased in volume following osimertinib treatment, PC-9*BIM*$^{EL-/-}$ xenograft tumors continued to grow, albeit more slowly (Fig. 5A and Supplementary Fig. S5). However, the combination of osimertinib with vorinostat led to a significant reduction in the size of PC-9*BIM*$^{EL-/-}$ xenograft tumors, without causing weight loss in treated mice (data not shown). In PC-9*BIM*$^{EL-/-}$ tumors, western blot analysis revealed that combined treatment with osimertinib and vorinostat markedly induced active BIM protein expression, and induced apoptosis as represented by increased cleaved caspase-3 (Fig. 5B).

Combined use of osimertinib and vorinostat induces apoptosis in *EGFR*-T790M mutation-positive NSCLC cells with the *BIM* deletion polymorphism

Studies have demonstrated that most patients with *EGFR*-mutated NSCLC and the *BIM* deletion polymorphism showed shorter PFS compared with those without the *BIM* deletion polymorphism (13). Since the *BIM* deletion polymorphism induces apoptosis resistance, but not growth impairment, to EGFR-TKI exposure, tumors with the *BIM* deletion polymorphism may be permissive for the acquisition of additional resistance mechanisms, as recently demonstrated in chronic myeloid leukemia (CML) (21). To assess this question, we established gefitinib-resistant cells from PC-9*BIM*$^{EL-/-}$ cells by continuous exposure to increasing concentrations of gefitinib and cloning by limiting dilution *in vitro*, which was designated as PC-9*BIM*$^{EL-/-}$GR. Interestingly, PC-9*BIM*$^{EL-/-}$GR cells acquired the *EGFR*-T790M mutation over time. While PC-9*BIM*$^{EL-/-}$GR cells were highly resistant to gefitinib in terms of cell viability, they had the same sensitivity to osimertinib compared with PC-9*BIM*$^{EL-/-}$ cells (Fig. 6A). Notably, while neither gefitinib, osimertinib nor vorinostat alone markedly induced apoptosis in PC-9*BIM*$^{EL-/-}$ and PC-9*BIM*$^{EL-/-}$GR cells, combined use of osimertinib and vorinostat markedly induced cell apoptosis in both PC-9*BIM*$^{EL-/-}$ and PC-9*BIM*$^{EL-/-}$GR cells (Fig. 6B). Western blotting demonstrated that while gefitinib did not reduce the expression of phosphorylated EGFR in PC-9*BIM*$^{EL-/-}$GR cells, osimertinib suppressed the phosphorylation of EGFR and its downstream kinases, AKT and ERK (Fig. 6C). Moreover, the combination of osimertinib and vorinostat upregulated both PARP and caspase-3 cleavage in PC-9*BIM*$^{EL-/-}$GR cells, indicating that apoptosis was induced in these tumor cells.

Discussion

The *BIM* deletion polymorphism is found in a significant proportion (~20%) of normal individuals of East Asian ethnicity (10), with the majority carrying one allele of the deletion polymorphism and only a minority who are homozygous (~0.5%) (10). Accordingly, native *EGFR*-mutated NSCLC cell lines that are homozygous for the *BIM* deletion polymorphism have yet to be described. In this study, we utilized the genetically-edited PC-9BIM$^{i2-/-}$ cells as a homozygous *BIM* deletion polymorphism-positive *EGFR*-mutant NSCLC cell line with which to explore the mechanism of HDAC activity (10). In PC-9BIM$^{i2-/-}$ cells, vorinostat decreased the ratio of exon 3 to exon 4 transcripts, increased active BIM protein expression, and resensitized cells to EGFR-TKI-induced apoptosis. These findings clearly indicate that vorinostat predominantly affects the deletion allele of *BIM* to overcome EGFR-TKI resistance, and also provides a rationale of combined treatment with vorinostat and EGFR-TKIs for patients with *EGFR*-mutated NSCLC who are homozygous for the *BIM* deletion polymorphism. In addition to the *BIM* deletion polymorphism in intron 2, several single nucleotide polymorphisms (SNPs) within the *BIM* locus were recently discovered (22, 23). A silent SNP (the T allele in the c465C>T) in exon 4 of *BIM* is reported to exist in ~30% of French individuals, and is associated with a delay in major molecular responses to imatinib in CML (22). Moreover, the *BIM* C29201T variant, located within the BH3-domain coding region, is reported to be associated with lower overall survival in children with acute lymphoblastic leukemia (23). Thus, further investigations are warranted to examine the effect of HDAC inhibitors on the target drug sensitivity of tumors with *BIM* SNPs.

HDACs can affect alternative mRNA splicing (24-26). For instance, the Hu proteins are thought to regulate pre-mRNA splicing through HDAC2 inhibition, which in turn modulates chromatin structures to alter splicing of NF1 in HeLa cells (27). The inhibition of HDAC1 but not HDAC2 is also important for the alternative splicing of fibronectin in HeLa cells (28). A recent study revealed that HDAC1 and HDAC2 co-purified with the U2 small nuclear ribonucleoprotein splicing factor, and that knockdown of these two deacetylases but not that of HDAC3 modified the splicing patterns of CD44 (29). These reports suggest that the different HDACs differentially regulate alternative splicing of specific pre-mRNAs. We here report that HDAC3 inhibition plays pivotal role on the alternative splicing of *BIM* caused by vorinostat. This is consistent with the results of Hnilicova et al. (28), who showed that HDAC inhibition by NaB did not change the splicing pattern in *BIM*, and which we reason is because NaB has much weaker HDAC3 inhibitory activity than vorinostat (30). While

HDAC3 is reported to have multiple functions in stem cell differentiation, embryonic cardiovascular development, and endothelial cell differentiation and integrity maintenance (31), the role of HDAC3 in alternative splicing is virtually unknown, as opposed to HDAC1 or HDAC2. Previous reports have documented that HDACs play a role in the expression of micro RNAs (miR) (32-34), and that micro RNAs regulate alternative splicing (35-37), suggesting that the influence of HDAC3 in splicing might be indirect. Specifically, Chen et al. reported that knockdown of *HDAC*3 up-regulated the expression of miR-15a and miR-16-1, which are important suppressors that modulate BCL-2 and other molecules (38). While we have established HDAC3 inhibition as important in the alternative splicing of *BIM* in deletion-positive *EGFR*-mutated NSCLC, the precise mechanism by which it does so needs to be further elucidated.

We observed that tumors of *BIM* deletion polymorphism-positive *EGFR*-mutated NSCLC cells were stable in size during EGFR-TKI treatment, indicating that the acquisition of additional resistance mechanisms is necessary for tumor enlargement during EGFR-TKI treatment. *EGFR*-T790M is the most frequent resistance mechanism detected in patients with *EGFR*-mutated NSCLC who are refractory to reversible EGFR-TKI treatment (4). In PC-9*BIM*$^{\Delta 2-/-}$GR cells, we detected the *EGFR*-T790M mutation which allows tumor cell growth even in the presence of gefitinib *in vitro*. Therefore, we speculate that T790M may be detected in a certain population of patients with *BIM* deletion-positive NSCLC harboring *EGFR* mutations who fail to respond to reversible EGFR-TKI therapy. *EGFR*-T790M-positive resistant tumors can occur either by selection of pre-existing *EGFR*-T790M-positive clones or via genetic evolution of initially *EGFR*-T790M-negative drug-tolerant cells (39, 40). In the latter case, drug-tolerant cells become a base for *de novo* evolution of the *EGFR*-T790M mutation (40). Since the cells with *BIM* deletion polymorphism are resistant to EGFR-TKI-induced apoptosis, these cells may become a base for *de novo* evolution of the *EGFR*-T790M mutation. Therefore, therapeutic strategies with vorinostat and EGFR-TKI to eradicate *BIM* deletion polymorphism-positive apoptosis-resistant cells may be useful for preventing the acquisition of the *EGFR*-T790M mutation in NSCLC. We are now conducting a phase I trial (NCT02296125) to assess the feasibility of combined treatment with vorinostat and gefitinib in *BIM* deletion polymorphism-positive *EGFR*-mutated NSCLC.

Third-generation EGFR-TKIs, including osimertinib, show high activity against T790M-positive *EGFR*-mutated NSCLC, but most patients subsequently develop resistance to this class of inhibitors (7, 41). Recent studies demonstrated that the C797S mutation in *EGFR* exon 20 is acquired in ~20% of osimertinib resistant cases (42). In

nearly half of cases who acquired resistance to third-generation EGFR-TKIs, tumors lose the T790M mutation and acquired other resistance mechanisms (42), including bypass track activation by *MET* amplification (43, 44) or *HER2* amplification (43), and small cell transformation (45). We here report that *BIM* deletion polymorphism is one of the mechanisms that cause apoptosis resistance to osimertinib in *EGFR*-mutated NSCLC cells with or without T790M. Since the *BIM* deletion polymorphism is associated with shorter PFS in patients with *EGFR*-mutated NSCLC who were treated with first-generation EGFR-TKIs, it may also be associated with worse outcomes for osimertinib-treated *EGFR*-T790M-positive patients. On the other hand, Lee et al. reported that the *BIM* polymorphism was not a predictive biomarker of EGFR-TKI resistance (46). Prospective studies with a larger number of cases will be necessary in the future. An ongoing phase III trial is currently comparing osimertinib and gefitinib as the first line treatment for *EGFR*-mutated NSCLC (NCT02296125). The results of this trial may indicate that osimertinib might be used as a first-line treatment for *EGFR*-mutated NSCLC in the future. If it is the case, elucidation of the resistance mechanisms to first-line osimertinib treatment in T790M-negative *EGFR*-mutated NSCLC would become more clinically important.

In summary, the present study demonstrated that the combination of vorinostat and osimertinib can be used to overcome osimertinib-resistance in *EGFR*-mutated NSCLC, which are either heterozygous or homozygous for the *BIM* deletion polymorphism, both *in vitro* and *in vivo*. Notably, HDAC3 inhibition by vorinostat plays a crucial role in apoptosis induction via promoting transcription and modulating alternative splicing to up-regulate active BIM protein in *BIM* deletion polymorphism-positive *EGFR*-mutated NSCLC cells. Furthermore, acquisition of the *EGFR*-T790M mutation allows *BIM* deletion polymorphism-positive *EGFR*-mutated NSCLC cells to grow in the presence of gefitinib, and combined use of vorinostat with osimertinib could induce apoptosis even when *BIM* deletion polymorphism-positive *EGFR*-mutated NSCLC cells acquire the T790M mutation. These findings illustrate the importance of developing HDAC3-selective inhibitors, and provide a rationale for their combined use with osimertinib to treat lung cancer with *EGFR* mutations and the *BIM* deletion polymorphism.

Legends for figures

Figure 1. NSCLC cell lines with *EGFR* mutations and *BIM* deletion polymorphism show apoptosis resistance to the second- and third-generation EGFR-TKIs. A, Gel

electrophoresis of PCR products from the three *EGFR*-mutated NSCLC cell lines. PCR product sizes for wild type (w) and deletion (d) alleles are 362 bp and 284 bp, respectively. B, Apoptosis determined by flow cytometry with PE Annexin V staining in PC-9 cells, PC-3 cells, and PC-9*BIM*$^{\Delta 2/-}$ cells treated with gefitinib (1 μmol/L), afatinib (1 μmol/L), and osimertinib (1 μmol/L) for 24 hours. *, $P < 0.05$ PC-3 or PC-9*BIM*$^{\Delta 2/-}$ versus PC-9 cells. All graph bars show mean values ± SD. C, Protein expression detected by western blotting in PC-9 cells (left), PC-3 cells (middle), and PC-9*BIM*$^{\Delta 2/-}$ cells (right), incubated with gefitinib (1 μmol/L), afatinib (1 μmol/L), or osimertinib (1 μmol/L), for 24 hours. D, Protein expression in PC-9 cells transfected by siRNA control (scramble) or *BIM* siRNA (si*BIM*) which were treated with each compound (1 μmol/L) for 24 hours.

The data shown are representative of at least three experiments with similar results.

Figure 2. Vorinostat overcomes apoptosis resistance to second- and third-generation EGFR-TKIs via active BIM protein expression. A, Protein expression by western blotting in PC-3 cells and PC-9*BIM*$^{\Delta 2/-}$ cells treated with gefitinib (1 μmol/L), afatinib (1 μmol/L), and osimertinib (1 μmol/L) and/or vorinostat (3 μmol/L) for 24 hours. B, Apoptosis determined by flow cytometry with PE Annexin V staining in PC-9*BIM*$^{\Delta 2/-}$ cells transfected with control (scramble) or BIM specific siRNA (si*BIM*) and then treated for 12 hours with EGFR-TKIs (1 μmol/L) and vorinostat (3 μmol/L).

The data shown are representative of at least three experiments with similar results.

Figure 3. HDAC3 plays a crucial role in the promotion of active *BIM* transcription. A, Western blotting of PC-9*BIM*$^{\Delta 2/-}$ cells treated with siRNA targeting *HDAC* 1, 2, 3, and 6 for 48 hours. B, Amounts of transcripts containing *BIM* exon 4 after each *HDAC*s siRNA transfection determined by RT-PCR. *, $P < 0.05$ siRNA control (scramble) or *HDAC*2 siRNA (si*HDAC*2) versus *HDAC*3 siRNA (si*HDAC*3). C, Western blotting of PC-9*BIM*$^{\Delta 2/-}$cells and PC-3 cells with/without *HDAC*3 knockdown were treated with osimertinib (1 μmol/L) for 24 hours. D, Expression of BIM and apoptosis-related proteins in PC-9*BIM*$^{\Delta 2/-}$ cells treated by osimertinib (1 μmol/L) with/without vorinostat (3 μmol/L) or droxinostat (3 μmol/L).

The data shown are representative of at least three experiments with similar results.

Figure 4. HDAC3 inhibition modulates alternative splicing of *BIM* in *EGFR*-mutated NSCLC cells which are homozygous for the *BIM* deletion polymorphism. A, Expression of BIM mRNA variants containing exon 2A, 3, or 4 in PC-9*BIM*$^{\Delta 2/-}$ cells treated by vorinostat (3 μmol/L) for 12 hours. B, Ratio of exon 3-containing transcripts to exon

4-containing transcripts in PC-9*BIM*$^{\Delta 2/-}$ cells. The mRNA expression were measured by RT-PCR and normalized to actin. *, $P < 0.05$ versus control. C, Ratio of exon 3 to exon 4 transcripts in PC-9*BIM*$^{\Delta 2/-}$ cells transfected with siRNA for each *HDAC*. *, $P < 0.05$ siRNA control (scramble) or *HDAC*1 siRNA (si*HDAC*1) versus *HDAC*3 siRNA (si*HDAC*3).

Data are expressed as the mean ± SD from three independent experiments.

Figure 5. Combined treatment with osimertinib and vorinostat regresses tumors which are homozygous for the *BIM* deletion polymorphism. A, Percentage change in tumor volume after 14 days of treatment in PC-9 (red and blue bar) and PC-9*BIM*$^{\Delta 2/-}$ (red, green, blue and yellow bar) xenografts. Nude mice bearing the xenografts were treated with 5 mg/kg of osimertinib and/or 40 mg/kg of vorinostat once daily. B, Protein expression of PC-9*BIM*$^{\Delta 2/-}$ tumor xenografts determined by western blotting. The xenografts were resected from mice treated with each drug for 4 days.

Figure 6. Combined use of osimertinib and vorinostat induces apoptosis in *EGFR*-T790M mutation-positive NSCLC cells with *BIM* deletion polymorphism. A, PC-9*BIM*$^{\Delta 2/-}$ or PC-9*BIM*$^{\Delta 2/-}$ GR cells were treated with gefitinib or osimertinib, and cell viability was determined after 72 hours by MTT assay. Data shown are representative of at least three independent experiments. The data shown are the mean ± SD of triplicate cultures. B, PC-9 cells, PC-9*BIM*$^{\Delta 2/-}$ cells, and PC-9*BIM*$^{\Delta 2/-}$ GR cells were treated with gefitinib (1 μmol/L), osimertinib (1 μmol/L), vorinostat (3 μmol/L), or a combination of osimertinib and vorinostat for 24 hours. Cell apoptosis was detected by Annexin V and 7-AAD staining. *, $P < 0.05$ for osimertinib versus osimertinib+vorinostat in PC-9*BIM*$^{\Delta 2/-}$ cells or PC-9*BIM*$^{\Delta 2/-}$ GR cells. All graph bars show mean values ± SD. C, Western blotting of PC-9*BIM*$^{\Delta 2/-}$ GR cells treated with gefitinib (1 μmol/L), osimertinib (1 μmol/L), and/or vorinostat (3 μmol/L) for 24 hours.

References

1. Maemondo M, Inoue A, Kobayashi K, Sugawara S, Oizumi S, Isobe H, et al. Gefitinib or chemotherapy for non-small-cell lung cancer with mutated EGFR. The New England journal of medicine. 2010;362(25):2380-8.
2. Rosell R, Carcereny E, Gervais R, Vergnenegre A, Massuti B, Felip E, et al. Erlotinib versus standard chemotherapy as first-line treatment for European patients with advanced EGFR mutation-positive non-small-cell lung cancer (EURTAC): a multicentre, open-label, randomised phase 3 trial. The Lancet Oncology. 2012;13(3):239-46.
3. Kobayashi S, Boggon TJ, Dayaram T, Janne PA, Kocher O, Meyerson M, et al. EGFR mutation and resistance of non-small-cell lung cancer to gefitinib. The New England journal of medicine. 2005;352(8):786-92.
4. Pao W, Miller VA, Politi KA, Riely GJ, Somwar R, Zakowski MF, et al. Acquired resistance of lung adenocarcinomas to gefitinib or erlotinib is associated with a second mutation in the EGFR kinase domain. PLoS medicine. 2005;2(3):e73.
5. Ward RA, Anderton MJ, Ashton S, Bethel PA, Box M, Butterworth S, et al. Structure- and reactivity-based development of covalent inhibitors of the activating and gatekeeper mutant forms of the epidermal growth factor receptor (EGFR). Journal of medicinal chemistry. 2013;56(17):7025-48.
6. Katakami N, Atagi S, Goto K, Hida T, Horai T, Inoue A, et al. LUX-Lung 4: a phase II trial of afatinib in patients with advanced non-small-cell lung cancer who progressed during prior treatment with erlotinib, gefitinib, or both. Journal of clinical oncology : official journal of the American Society of Clinical Oncology. 2013;31(27):3335-41.
7. Janne PA, Yang JC, Kim DW, Planchard D, Ohe Y, Ramalingam SS, et al. AZD9291 in EGFR inhibitor-resistant non-small-cell lung cancer. The New England journal of medicine. 2015;372(18):1689-99.
8. Faber AC, Corcoran RB, Ebi H, Sequist LV, Waltman BA, Chung E, et al. BIM expression in treatment-naive cancers predicts responsiveness to kinase inhibitors. Cancer discovery. 2011;1(4):352-65.
9. Costa C, Molina MA, Drozdowskyj A, Gimenez-Capitan A, Bertran-Alamillo J, Karachaliou N, et al. The Impact of EGFR T790M Mutations and BIM mRNA Expression on Outcome in Patients with EGFR-Mutant NSCLC Treated with Erlotinib or Chemotherapy in the Randomized Phase III EURTAC Trial. Clinical cancer research : an official journal of the American Association for Cancer Research. 2014;20(7):2001-10.
10. Ng KP, Hillmer AM, Chuah CT, Juan WC, Ko TK, Teo AS, et al. A common BIM deletion polymorphism mediates intrinsic resistance and inferior responses to tyrosine kinase

579 inhibitors in cancer. Nature medicine. 2012;18(4):521-8.
580 11.Cardona A RL, Wills B, Arrieta O. BIM deletion polymorphisms in Hispanic patients
581 with non-small cell lung cancer carriers of EGFR mutations. Oncotarget.
582 2016;7(42):68933-42.
583 12.Juan WC, Roca X, Ong ST. Identification of cis-acting elements and splicing factors
584 involved in the regulation of BIM Pre-mRNA splicing. PloS one. 2014;9(4):e95210.
585 13.Nie W, Tao X, Wei H, Chen WS, Li B. The BIM deletion polymorphism is a prognostic
586 biomarker of EGFR-TKIs response in NSCLC: A systematic review and meta-analysis.
587 Oncotarget. 2015;6(28):25696-700.
588 14.Nakagawa T, Takeuchi S, Yamada T, Ebi H, Sano T, Nanjo S, et al. EGFR-TKI resistance
589 due to BIM polymorphism can be circumvented in combination with HDAC inhibition.
590 Cancer research. 2013;73(8):2428-34.
591 15.Marks PA, Xu WS. Histone deacetylase inhibitors: Potential in cancer therapy. Journal of
592 cellular biochemistry. 2009;107(4):600-8.
593 16.Duvic M, Talpur R, Ni X, Zhang C, Hazarika P, Kelly C, et al. Phase 2 trial of oral
594 vorinostat (suberoylanilide hydroxamic acid, SAHA) for refractory cutaneous T-cell
595 lymphoma (CTCL). Blood. 2007;109(1):31-9.
596 17.Wood TE, Dalili S, Simpson CD, Sukhai MA, Hurren R, Anyiwe K, et al. Selective
597 inhibition of histone deacetylases sensitizes malignant cells to death receptor ligands.
598 Molecular cancer therapeutics. 2010;9(1):246-56.
599 18.Richon VM, Emiliani S, Verdin E, Webb Y, Breslow R, Rifkind RA, et al. A class of hybrid
600 polar inducers of transformed cell differentiation inhibits histone deacetylases.
601 Proceedings of the National Academy of Sciences of the United States of America.
602 1998;95(6):3003-7.
603 19.Plumb JA, Finn PW, Williams RJ, Bandara MJ, Romero MR, Watkins CJ, et al.
604 Pharmacodynamic response and inhibition of growth of human tumor xenografts by the
605 novel histone deacetylase inhibitor PXD101. Molecular cancer therapeutics.
606 2003;2(8):721-8.
607 20.Malvaez M, McQuown SC, Rogge GA, Astarabadi M, Jacques V, Carreiro S, et al.
608 HDAC3-selective inhibitor enhances extinction of cocaine-seeking behavior in a
609 persistent manner. Proceedings of the National Academy of Sciences of the United States
610 of America. 2013;110(7):2647-52.
611 21.Ko TK, Chin HS, Chuah CT, Huang JW, Ng KP, Khaw SL, et al. The BIM deletion
612 polymorphism: A paradigm of a permissive interaction between germline and acquired
613 TKI resistance factors in chronic myeloid leukemia. Oncotarget. 2016;7(3):2721-33.
614 22.Augis V, Airiau K, Josselin M, Turcq B, Mahon FX, Belloc F. A single nucleotide

615 polymorphism in cBIM is associated with a slower achievement of major molecular
616 response in chronic myeloid leukaemia treated with imatinib. PloS one.
617 2013;8(11):e78582.
618 23.Gagne V, Rousseau J, Labuda M, Sharif-Askari B, Brukner I, Laverdiere C, et al. Bim
619 polymorphisms: influence on function and response to treatment in children with acute
620 lymphoblastic leukemia. Clinical cancer research : an official journal of the American
621 Association for Cancer Research. 2013;19(18):5240-9.
622 24.Schor IE, Rascovan N, Pelisch F, Allo M, Kornblihtt AR. Neuronal cell depolarization
623 induces intragenic chromatin modifications affecting NCAM alternative splicing.
624 Proceedings of the National Academy of Sciences of the United States of America.
625 2009;106(11):4325-30.
626 25.Nakka KK, Chaudhary N, Joshi S, Bhat J, Singh K, Chatterjee S, et al. Nuclear
627 matrix-associated protein SMAR1 regulates alternative splicing via HDAC6-mediated
628 deacetylation of Sam68. Proceedings of the National Academy of Sciences of the United
629 States of America. 2015;112(26):E3374-83.
630 26.Khan DH, Gonzalez C, Tailor N, Hamedani MK, Leygue E, Davie JR. Dynamic Histone
631 Acetylation of H3K4me3 Nucleosome Regulates MCL1 Pre-mRNA Splicing. J Cell
632 Physiol. 2016.
633 27.Zhou HL, Hinman MN, Barron VA, Geng C, Zhou G, Luo G, et al. Hu proteins regulate
634 alternative splicing by inducing localized histone hyperacetylation in an RNA-dependent
635 manner. Proceedings of the National Academy of Sciences of the United States of
636 America. 2011;108(36):E627-35.
637 28.Hnilicova J, Hozeifi S, Duskova E, Icha J, Tomankova T, Stanek D. Histone deacetylase
638 activity modulates alternative splicing. PloS one. 2011;6(2):e16727.
639 29.Allemand E, Myers MP, Garcia-Bernardo J, Harel-Bellan A, Krainer AR, Muchardt C. A
640 Broad Set of Chromatin Factors Influences Splicing. PLoS genetics. 2016;12(9):e1006318.
641 30.Bradner JE, Mak R, Tanguturi SK, Mazitschek R, Haggarty SJ, Ross K, et al. Chemical
642 genetic strategy identifies histone deacetylase 1 (HDAC1) and HDAC2 as therapeutic
643 targets in sickle cell disease. Proceedings of the National Academy of Sciences of the
644 United States of America. 2010;107(28):12617-22.
645 31.Zeng L, Wang G, Ummarino D, Margariti A, Xu Q, Xiao Q, et al. Histone deacetylase 3
646 unconventional splicing mediates endothelial-to-mesenchymal transition through
647 transforming growth factor beta2. The Journal of biological chemistry.
648 2013;288(44):31853-66.
649 32.Zhou R, Gong AY, Chen D, Miller RE, Eischeid AN, Chen XM. Histone deacetylases and
650 NF-kB signaling coordinate expression of CX3CL1 in epithelial cells in response to

651 microbial challenge by suppressing miR-424 and miR-503. PloS one. 2013;8(5):e65153.
652 33.Kaluza D, Kroll J, Gesierich S, Manavski Y, Boeckel JN, Doebele C, et al. Histone
653 deacetylase 9 promotes angiogenesis by targeting the antiangiogenic microRNA-17-92
654 cluster in endothelial cells. Arteriosclerosis, thrombosis, and vascular biology.
655 2013;33(3):533-43.
656 34.Chatterjee N, Wang WL, Conklin T, Chittur S, Tenniswood M. Histone deacetylase
657 inhibitors modulate miRNA and mRNA expression, block metaphase, and induce
658 apoptosis in inflammatory breast cancer cells. Cancer biology & therapy.
659 2013;14(7):658-71.
660 35.Cardinali B, Cappella M, Provenzano C, Garcia-Manteiga JM, Lazarevic D, Cittaro D, et
661 al. MicroRNA-222 regulates muscle alternative splicing through Rbm24 during
662 differentiation of skeletal muscle cells. Cell death & disease. 2016;7:e2086.
663 36.Zhang BW, Cai HF, Wei XF, Sun JJ, Lan XY, Lei CZ, et al. miR-30-5p Regulates Muscle
664 Differentiation and Alternative Splicing of Muscle-Related Genes by Targeting MBNL.
665 International journal of molecular sciences. 2016;17(2).
666 37.Kalantari R, Chiang CM, Corey DR. Regulation of mammalian transcription and splicing
667 by Nuclear RNAi. Nucleic acids research. 2016;44(2):524-37.
668 38.Chen CQ, Chen CS, Chen JJ, Zhou LP, Xu HL, Jin WW, et al. Histone deacetylases
669 inhibitor trichostatin A increases the expression of Dleu2/miR-15a/16-1 via HDAC3 in
670 non-small cell lung cancer. Molecular and cellular biochemistry. 2013;383(1-2):137-48.
671 39.Inukai M, Toyooka S, Ito S, Asano H, Ichihara S, Soh J, et al. Presence of epidermal
672 growth factor receptor gene T790M mutation as a minor clone in non-small cell lung
673 cancer. Cancer research. 2006;66(16):7854-8.
674 40.Hata AN, Niederst MJ, Archibald HL, Gomez-Caraballo M, Siddiqui FM, Mulvey HE, et
675 al. Tumor cells can follow distinct evolutionary paths to become resistant to epidermal
676 growth factor receptor inhibition. Nature medicine. 2016;22(3):262-9.
677 41.Sequist LV, Rolfe L, Allen AR. Rociletinib in EGFR-Mutated Non-Small-Cell Lung
678 Cancer. The New England journal of medicine. 2015;373(6):578-9.
679 42.Thress KS, Paweletz CP, Felip E, Cho BC, Stetson D, Dougherty B, et al. Acquired EGFR
680 C797S mutation mediates resistance to AZD9291 in non-small cell lung cancer harboring
681 EGFR T790M. Nature medicine. 2015;21(6):560-2.
682 43.Planchard D, Loriot Y, Andre F, Gobert A, Auger N, Lacroix L, et al. EGFR-independent
683 mechanisms of acquired resistance to AZD9291 in EGFR T790M-positive NSCLC
684 patients. Annals of oncology : official journal of the European Society for Medical
685 Oncology / ESMO. 2015;26(10):2073-8.
686 44.Ou SH, Agarwal N, Ali SM. High MET amplification level as a resistance mechanism to

687 osimertinib (AZD9291) in a patient that symptomatically responded to crizotinib
688 treatment post-osimertinib progression. Lung cancer (Amsterdam, Netherlands).
689 2016;98:59-61.
690 45.Piotrowska Z, Niederst MJ, Karlovich CA, Wakelee HA, Neal JW, Mino-Kenudson M, et
691 al. Heterogeneity Underlies the Emergence of EGFRT790 Wild-Type Clones Following
692 Treatment of T790M-Positive Cancers with a Third-Generation EGFR Inhibitor. Cancer
693 discovery. 2015;5(7):713-22.
694 46.Lee JY, Ku BM, Lim SH, Lee MY, Kim H, Kim M, et al. The BIM Deletion Polymorphism
695 and its Clinical Implication in Patients with EGFR-Mutant Non-Small-Cell Lung Cancer
696 Treated with EGFR Tyrosine Kinase Inhibitors. Journal of thoracic oncology : official
697 publication of the International Association for the Study of Lung Cancer.
698 2015;10(6):903-9.
699

Figure 1

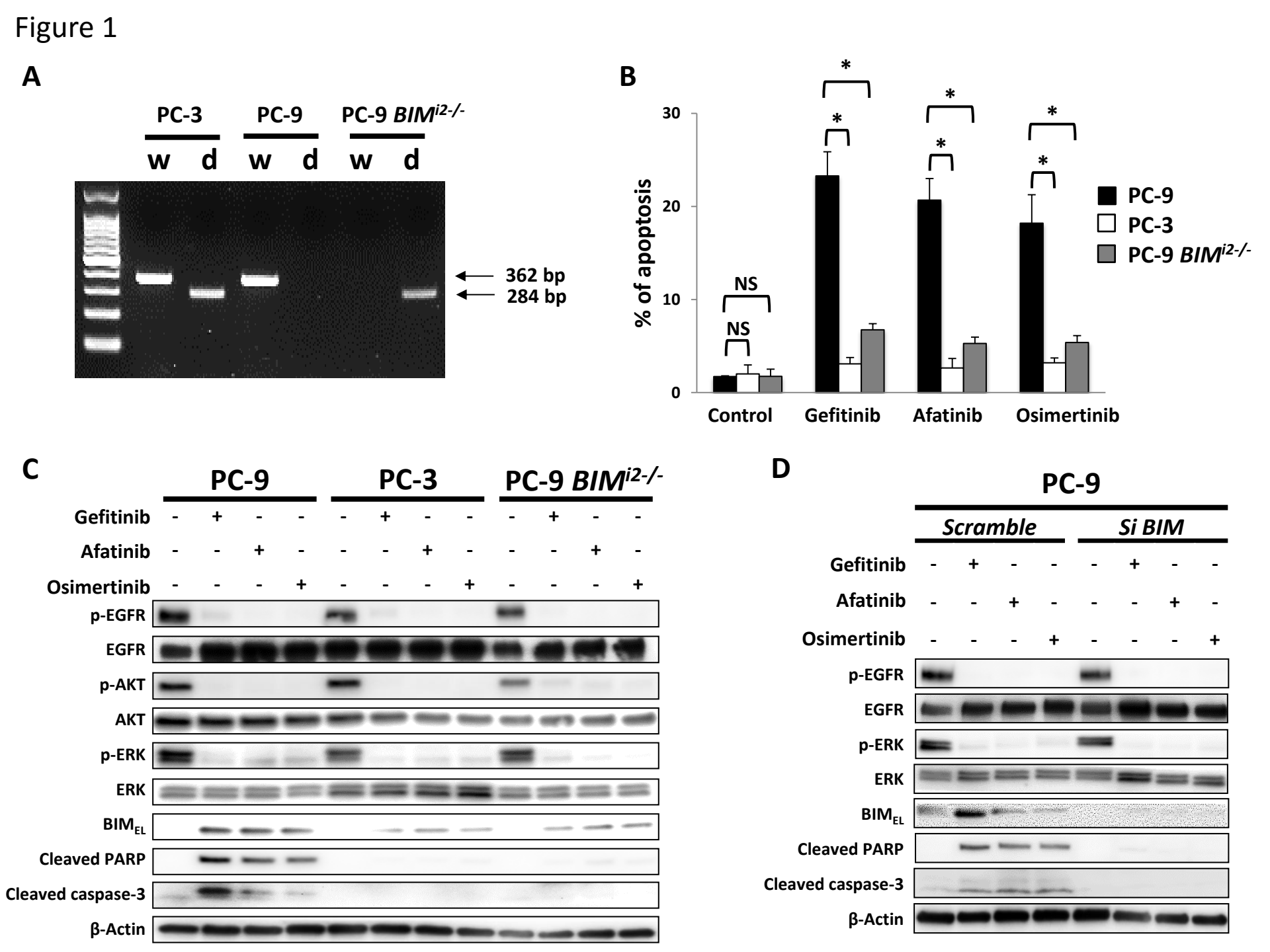
A
PC-3
PC-9
PC-9 BIMi2-/-
w d w d w d
362 bp
284 bp
B
% of apoptosis
30
20
10
0
NS
NS
*
PC-9
PC-3
PC-9 BIMi2-/-
Control
Gefitinib
Afatinib
Osimertinib
C
PC-9
PC-3
PC-9 BIMi2-/-
Gefitinib
Afatinib
Osimertinib
p-EGFR
EGFR
p-AKT
AKT
p-ERK
ERK
BIMEL
Cleaved PARP
Cleaved caspase-3
β-Actin
D
PC-9
Scramble
Si BIM
Gefitinib
Afatinib
Osimertinib
p-EGFR
EGFR
p-ERK
ERK
BIMEL
Cleaved PARP
Cleaved caspase-3
β-Actin

Figure 2

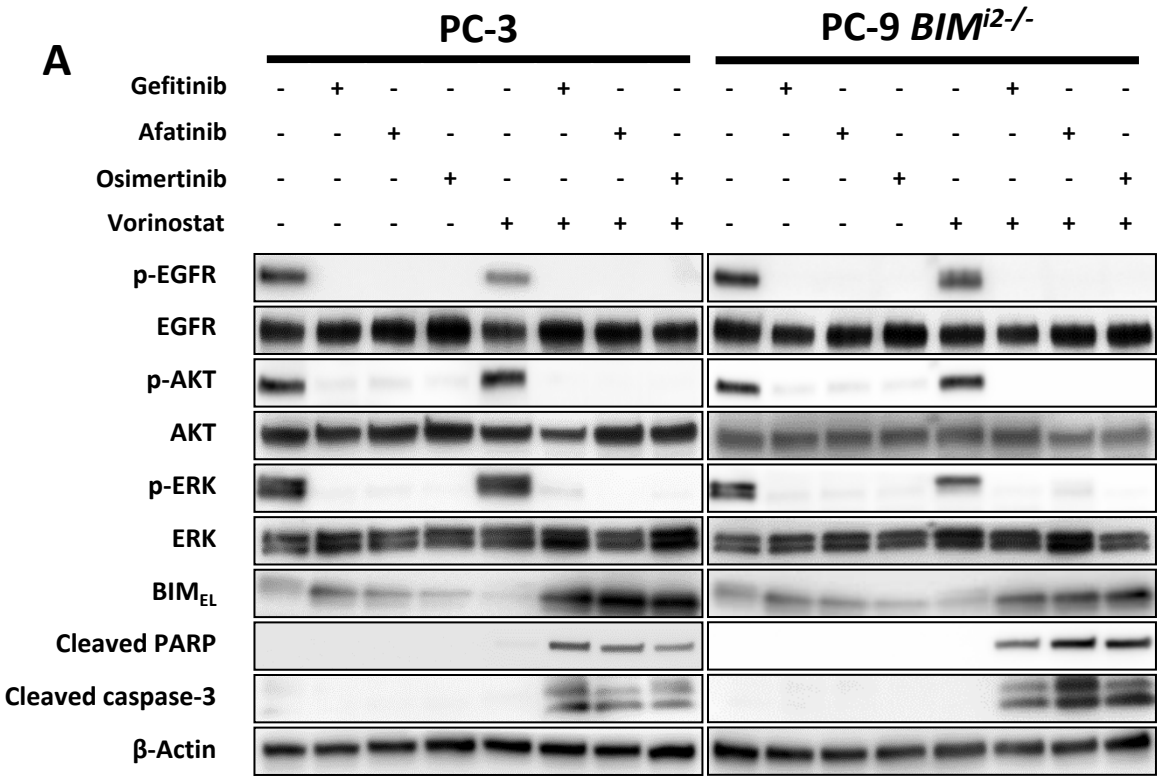
A
PC-3
PC-9 BIMi2-/-
Gefitinib
Afatinib
Osimertinib
Vorinostat
p-EGFR
EGFR
p-AKT
AKT
p-ERK
ERK
BIMEL
Cleaved PARP
Cleaved caspase-3
β-Actin

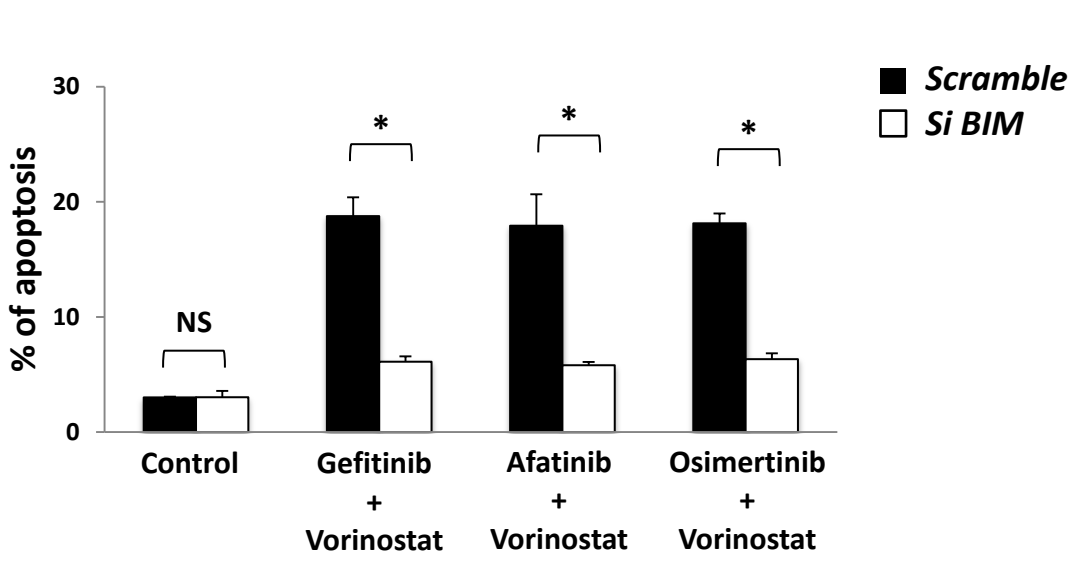
B
Scramble
Si BIM
% of apoptosis
30
20
10
0
NS
*
*
*
Control
Gefitinib + Vorinostat
Afatinib + Vorinostat
Osimertinib + Vorinostat

Figure 3

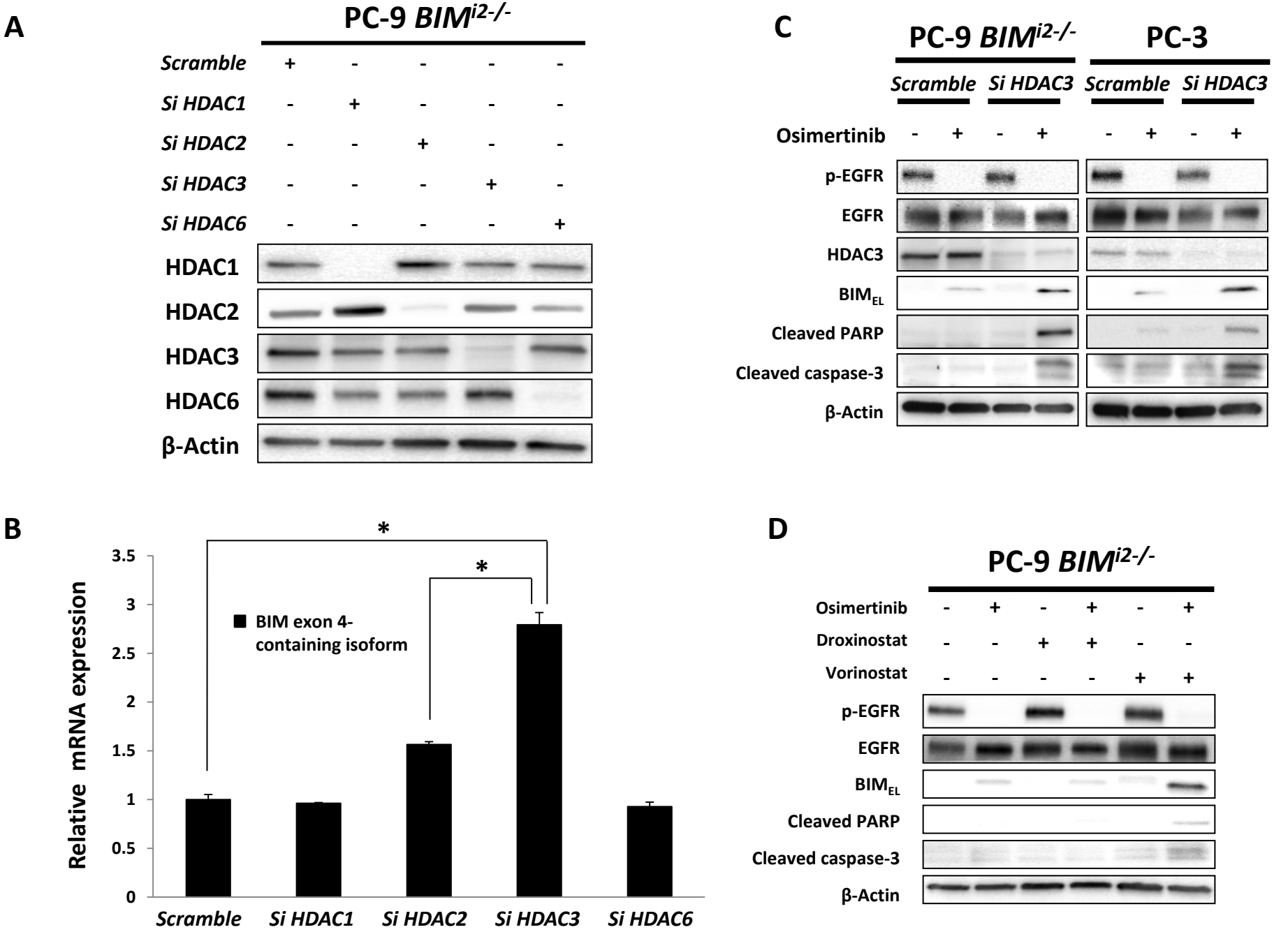
A
PC-9 BIMi2-/-
Scramble
Si HDAC1
Si HDAC2
Si HDAC3
Si HDAC6
HDAC1
HDAC2
HDAC3
HDAC6
β-Actin
B
Relative mRNA expression
BIM exon 4-containing isoform
Scramble
Si HDAC1
Si HDAC2
Si HDAC3
Si HDAC6
C
PC-9 BIMi2-/-
PC-3
Scramble
Si HDAC3
Osimertinib
p-EGFR
EGFR
HDAC3
BIMEL
Cleaved PARP
Cleaved caspase-3
β-Actin
D
PC-9 BIMi2-/-
Osimertinib
Droxinostat
Vorinostat
p-EGFR
EGFR
BIMEL
Cleaved PARP
Cleaved caspase-3
β-Actin

Figure 4

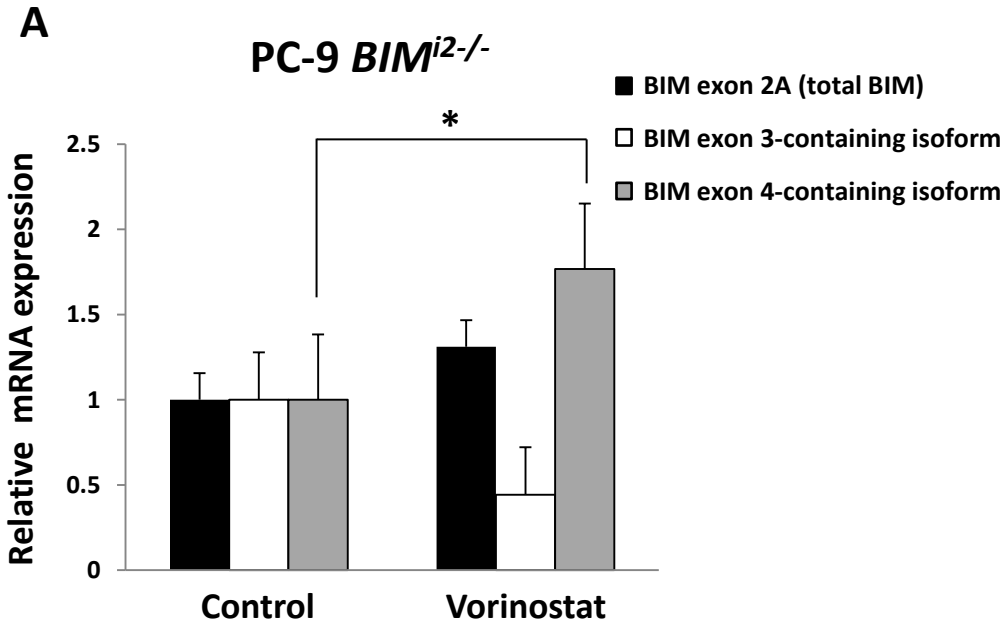
A
PC-9 BIMi2-/-
BIM exon 2A (total BIM)
BIM exon 3-containing isoform
BIM exon 4-containing isoform
Relative mRNA expression
2.5
2
1.5
1
0.5
0
*
Control
Vorinostat

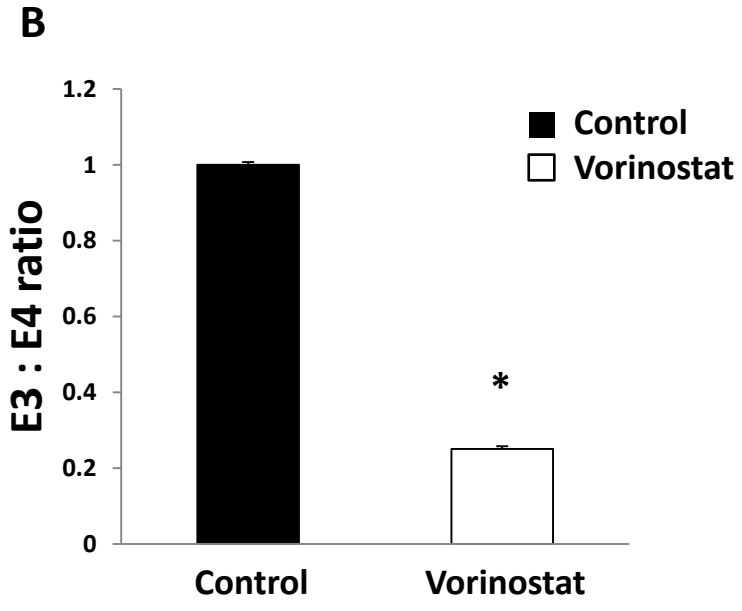
B
E3 : E4 ratio
1.2
1
0.8
0.6
0.4
0.2
0
Control
Vorinostat
*
Control
Vorinostat

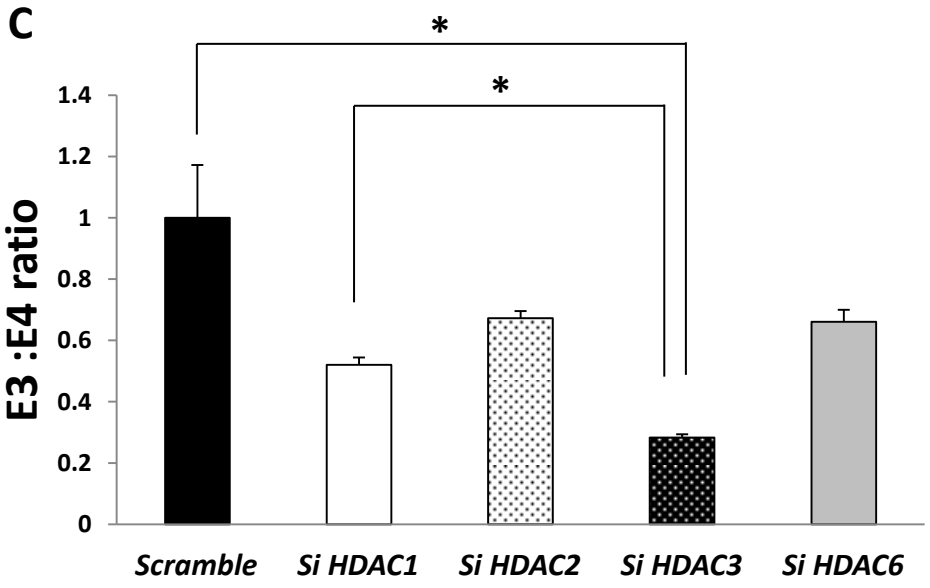
C
E3 :E4 ratio
1.4
1.2
1
0.8
0.6
0.4
0.2
0
*
*
Scramble
Si HDAC1
Si HDAC2
Si HDAC3
Si HDAC6

Figure 5

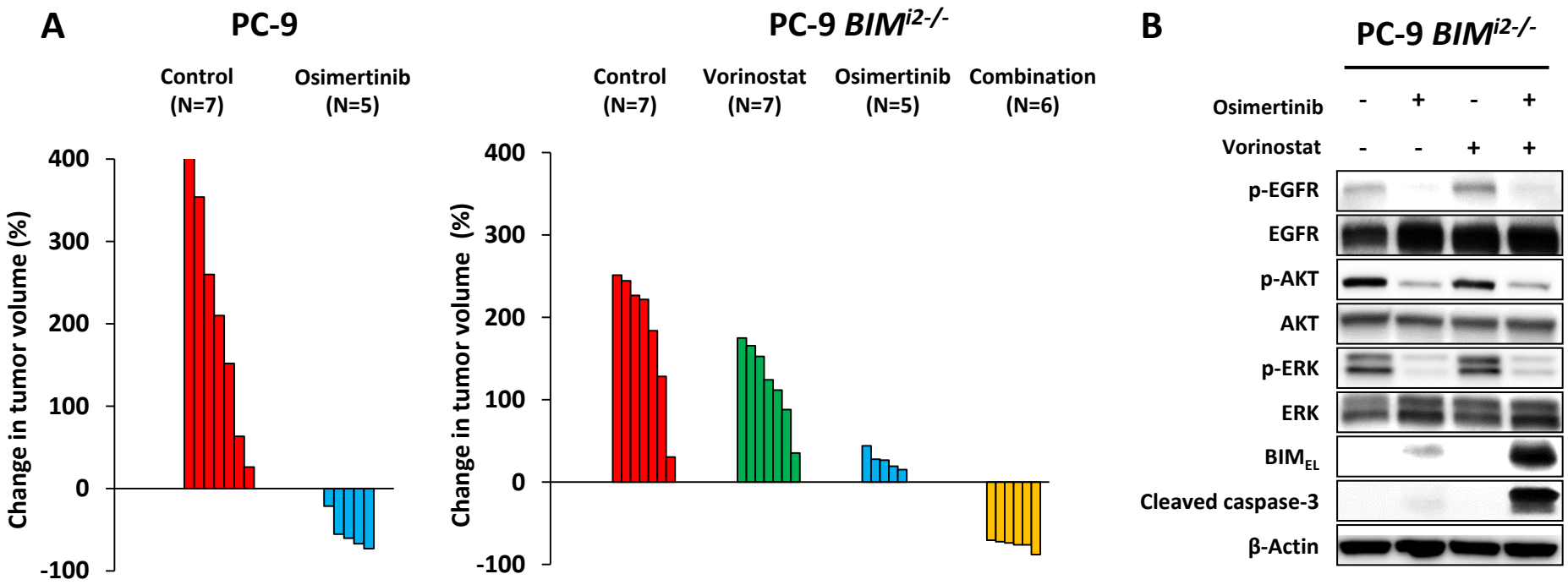
A
PC-9
Control (N=7)
Osimertinib (N=5)
Change in tumor volume (%)
400
300
200
100
0
-100
PC-9 BIMi2-/-
Control (N=7)
Vorinostat (N=7)
Osimertinib (N=5)
Combination (N=6)
B
PC-9 BIMi2-/-
Osimertinib - + - +
Vorinostat - - + +
p-EGFR
EGFR
p-AKT
AKT
p-ERK
ERK
BIMEL
Cleaved caspase-3
β-Actin

Figure 6

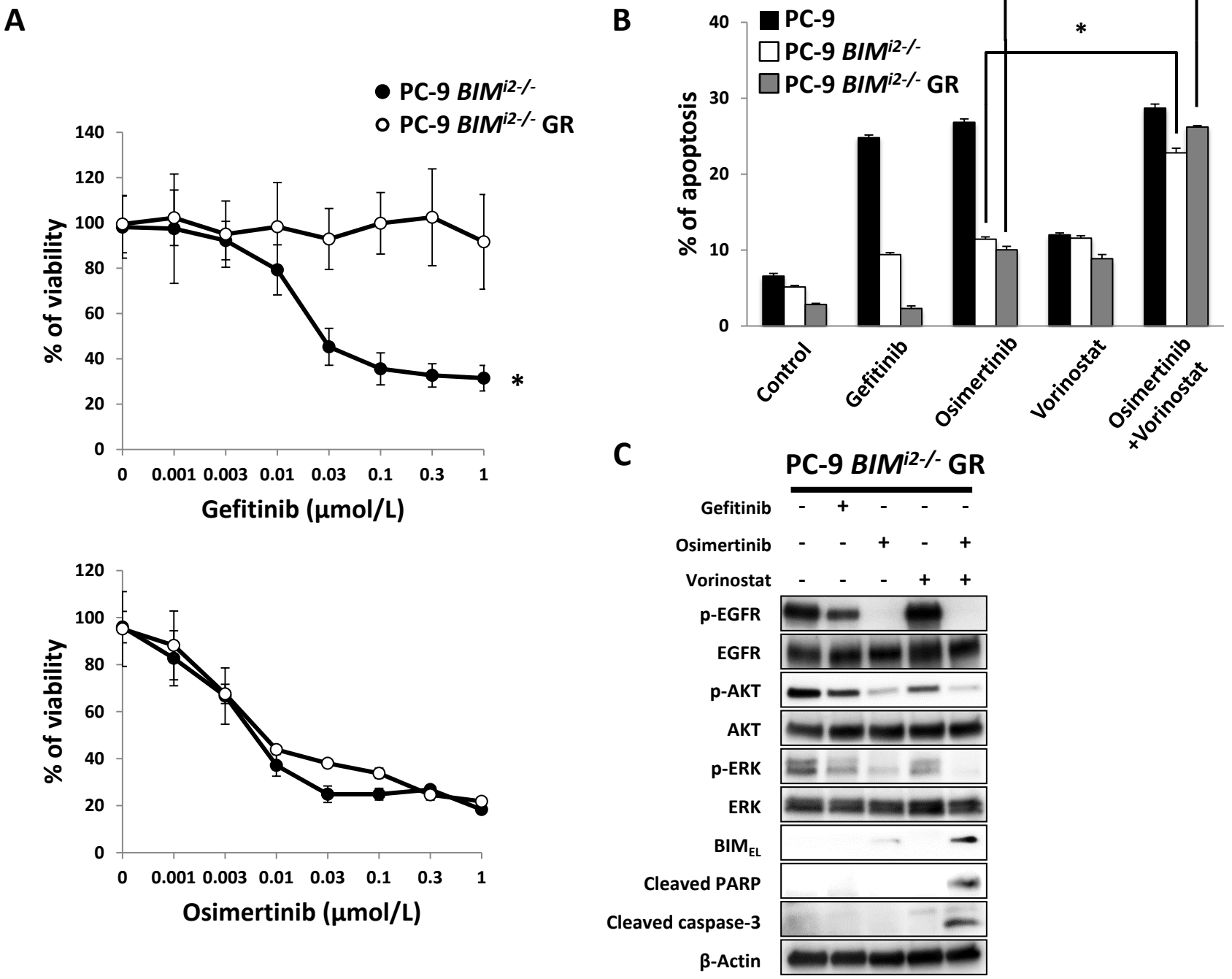
A
PC-9 BIMi2-/-
PC-9 BIMi2-/- GR
% of viability
Gefitinib (μmol/L)
Osimertinib (μmol/L)
B
PC-9
PC-9 BIMi2-/-
PC-9 BIMi2-/- GR
% of apoptosis
Control
Gefitinib
Osimertinib
Vorinostat
Osimertinib +Vorinostat
C
PC-9 BIMi2-/- GR
Gefitinib
Osimertinib
Vorinostat
p-EGFR
EGFR
p-AKT
AKT
p-ERK
ERK
BIMEL
Cleaved PARP
Cleaved caspase-3
β-Actin